

High resolution micro-XRF maps of iron oxides inside sensory dendrites of putative avian magnetoreceptors

This content has been downloaded from IOPscience. Please scroll down to see the full text.

2009 J. Phys.: Conf. Ser. 186 012084

(<http://iopscience.iop.org/1742-6596/186/1/012084>)

View [the table of contents for this issue](#), or go to the [journal homepage](#) for more

Download details:

IP Address: 146.175.11.141

This content was downloaded on 14/11/2013 at 17:12

Please note that [terms and conditions apply](#).

High resolution micro-XRF maps of iron oxides inside sensory dendrites of putative avian magnetoreceptors

G. Falkenberg^{1*}, Ge. Fleissner², Gue. Fleissner², K. Schuchardt², M. Kühbacher³, E. Chalmin⁴, K. Janssens⁵

¹ HASYLAB at DESY Hamburg, Germany

² Institute of Cell Biology and Neurosciences, Goethe-University Frankfurt a. M., Germany

³ Department of Molecular Trace Element Research in the Life Sciences, Helmholtz Centre Berlin for Materials and Energy, Berlin, Germany

⁴ ID21 ESRF, Grenoble, France

⁵ Department of Chemistry, University Antwerp, Belgium

Abstract. Iron mineral containing sensory dendrites in the inner lining of the upper beak of homing pigeons [1] and various bird species [2] are the first candidate structures for an avian magnetic field receptor. A new concept of magnetoreception [3, 4] is based on detailed ultra-structural optical and electron microscopy analyses in combination with synchrotron radiation microscopic X-ray fluorescence analysis (micro-XRF) and microscopic X-ray absorption near edge structures (micro-XANES). Several behavioral experiments [5, 6] and first mathematical simulations [6] affirm our avian magnetoreceptor model. The iron minerals inside the dendrites are housed in three different subcellular compartments (bullets, platelets, vesicles), which could be clearly resolved and identified by electron microscopy on ultrathin sections [1, 3]. Micro-XRF and micro-XANES data obtained at HASYLAB beamline L added information about the elemental distribution and Fe speciation [3], but are averaged over the complete dendrite due to limited spatial resolution. Here we present recently performed micro-XRF maps with sub-micrometer resolution (ESRF ID21), which reveal for the first time subcellular structural information from almost bulk-like dendrite sample material. Due to the thickness of 30 μm the microarchitecture of the dendrites can be considered as undisturbed and artefacts introduced by sectioning might be widely reduced.

1. Introduction

Though magnetoreception could be established as a "sixth" sense in animals from different phyla mainly by behavioral tests, only little is known on the receptor- and neurophysiological basis of magnetoreception [for review 6]. This might be attributed to a principle lack of both: studies which apply receptorphysiological principles to a putative magnetoreceptor candidate and also critical physical check-ups concerning its function under natural conditions. Therefore, hypotheses rather than facts govern the field and basically two mechanisms are proposed as a basis for magnetic field guided orientation and possibly interact for a safe tool to find a distant goal [6]. A photopigment-based magnetoreceptor within the retina might provide a compass, an iron-mineral-based receptor within the beak could serve as a magnetometer. Experiments for testing the retinal magnetoreceptor are mainly behavioral tests or physical simulations of magnetic field effects on the assumed key molecule, cryptochrome. A detailed cellular localization and the nature of magnetic field induced receptor mechanisms are still unknown. In this paper, we will deal only with the second mechanism, the iron mineral based magnetoreception. In upper beaks of different bird species, homing pigeons, migratory and non-migratory birds, we could describe highly specialized sensory dendrites [1, 2, 3], which match all histological and physical prerequisites as the smallest units of a receptor system sensing the gradual changes of the Earth magnetic field [4]. But we still must specify the stimulus-response function¹ for a sound characterization of the physiological features and the biological meaning of this system. A major difficulty originates from the broad range of different dimensions (cm down to nm) of the particles and components involved and the unsolved question concerning e.g. their relative position: (1) Within the beak we find six areas (each about $300 \times 15 \times 15 \mu\text{m}^3$ wide) with multiple iron containing dendrites.

* To whom all correspondence should be addressed: gerald.falkenberg@desy.de

¹ Detailed knowledge of the putative threshold and saturation values as well as the dynamics of the proposed magnetoreceptor are indispensable for all further studies as inadequate stimuli might destroy or at least temporarily constrain the system and conceal its biological function.

The 3-dimensional arrangement of the dendrites within these areas indicates that they may form the structural basis for a 3-axial magnetometer. But how precise is their alignment? Is their a bias? Are the dendrites within the bilateral areas parallel to each other or tilted for a better spatial resolution? (2) So far, we have found all dendrites of identical shape and size ($20 \times 5 \mu\text{m}^2$) and equipped with the same iron containing compartments: 10-15 bullets (diameter $1 \mu\text{m}$), a vesicle (diameter $5 \mu\text{m}$) and two parallel sets of chains of crystals (each $1 \times 1 \times 0.1 \mu\text{m}^3$). But as we can observe all these particles in ultrathin sections only, we do not know their in situ alignment, which would be necessary to better evaluate the magnetic forces between the iron containing components. (3) The bullets consist of nanomagnets (about 4 to 7 nm). So far we do not have a precise idea of their assembly. Magnetic field effects may vary when they are free to move as single crystals compared to an organization in small interdependent chains.

All histological procedures and physicochemical analyses, which have been applied in our project before, provided either highly resolved details in ultrathin sections or rather coarse overviews in thick sections. By means of ID21 at ESRF we now have started pilot experiments with XRF-mappings combining both: in rather thick sections ($30 \mu\text{m}$)² - thus avoiding structural distortion by histological procedures - we have analyzed large dendritic areas of the skin with a high resolution, which would allow an identification of the microarchitecture. The lateral resolution is maintained because the Fe containing structures are much smaller than the section thickness. Further experiments might help to identify the specific iron oxides inside the dendrites and clearly discriminate them from the iron generally occurring within the surrounding tissue and blood capillaries.

2. Results and Discussion

In histological sections of the inner lining of the upper beak of a homing pigeon distinct areas, sensory dendrites, with high concentrations of iron could be found by means of Prussian Blue staining. This qualitative method has served as a preselection of samples, which were mapped by μ -XRF-methods for a quantitative analysis of the dendritic iron minerals [3]. XRF-mappings of $10 \mu\text{m}$ thick sections at beamline L at HASYLAB (DESY Hamburg) of an axonal bundle can depict different minerals, which are indicative for nervous tissue (e.g. Ca) colocalized with iron (Fe) concentrated at several sites (Fig. 1). But iron is also present all over the tissue strand (weak tint). Here we face two difficulties, when we try to specify the iron within distinct compartments: Due to the focal size (about $5 \mu\text{m}$) of the XRF-beam it is not (yet) possible to discriminate between the iron of certain particles (bullets or platelets with $1 \mu\text{m}$ diameter) within the sensory dendrite, which we assume as essential for magnetoreceptive function, and even individual dendrites are not resolved within the dendritic field. Iron regularly occurring in any other cellular compartment of the surrounding nervous and connective tissue cells as part of their iron metabolism, e.g. hemoglobin, cytochrome, ferritin will also add to the measurement.

At ID21 (ESRF) we were able to test thicker sections ($30 \mu\text{m}$) with higher resolution (Fig. 2). The μ -XRF-mappings now clearly show networks of iron containing structures, which resemble in their size and shape (5 to $20 \mu\text{m}$) the known sensory dendrites. For the first time this thick section also shows their microarchitecture with a main alignment of the dendrites in parallel to the rim of the nervous strand. Few dendrites, however, deviate from this direction in an angle of about $\pm 45^\circ$ (Fig. 2C). In our previous papers we have provided evidence that each dendrite may sense only one direction of the magnetic field [3, 4]. Several dendrites with a different alignment in the skin are necessary to enable the system to monitor different directions of the magnetic field. Previously, we could show six dendritic areas with a perpendicular orientation of the dendrites [3, 4]. But we did not know how strict or uniform this 3D-microarchitecture might be in situ, as all data so far stem from serial sections of the skin - with the disadvantage of an ambiguous distortion or displacement. Sensory systems, in general, avoid step-like stimulus-response functions, as this would yield an all-or-none signal and prevent a gradual excitation according to smooth changes of the adequate stimulus. Based on the ID21 data, we

² In previous papers [1,3] we have published the caveats of the processing of this material in detail, also the parallel investigation of unstained test sections in parallel to Prussian Blue stained control sections in order to find the relevant dendritic areas of the skin. For comparison, parallel sections were mapped at beamline L at HASYLAB and then inspected at ID21 at ESRF.

now predict that the entity of the iron containing dendrites deliver a transition curve with a shallow slope. The system may monitor gradual changes of the 3 axis of the earth magnetic field.

Further experiments at ID21 or similar X-ray microprobe beamlines will hopefully disclose the subcellular micro-architecture in greater detail, i.e. the relative position of the iron-containing compartments, once the analyses can be performed without a disintegration of the structural context, and also identify the specificity of iron minerals within single bullets, platelets or vesicles.

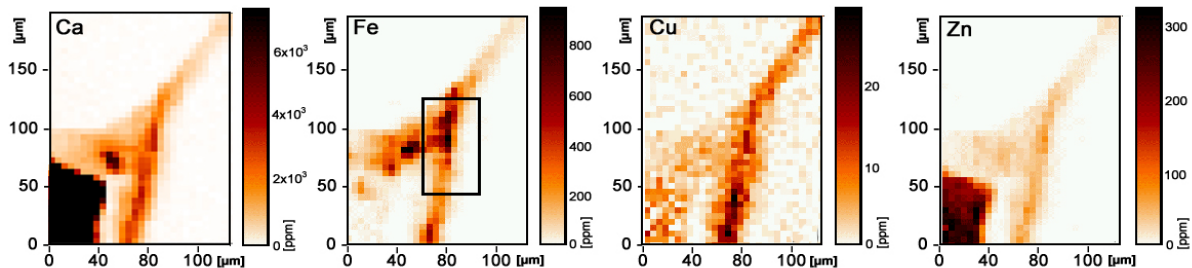


Fig. 1 Micro-XRF element mappings at beamline L at HASYLAB (beam size $5 \times 5 \mu\text{m}^2$, 1×10^{10} ph/s, 17 keV). The measurements confirm the distribution of Fe within or next to nervous tissue according to the distribution of Ca, Cu and Zn. [10 μm thick paraffin section, unstained. The Ca intensity color scale has been truncated at 1/20 of the maximum value. The square indicates the site of the ID21 measurements in a parallel section (see Fig. 2)].

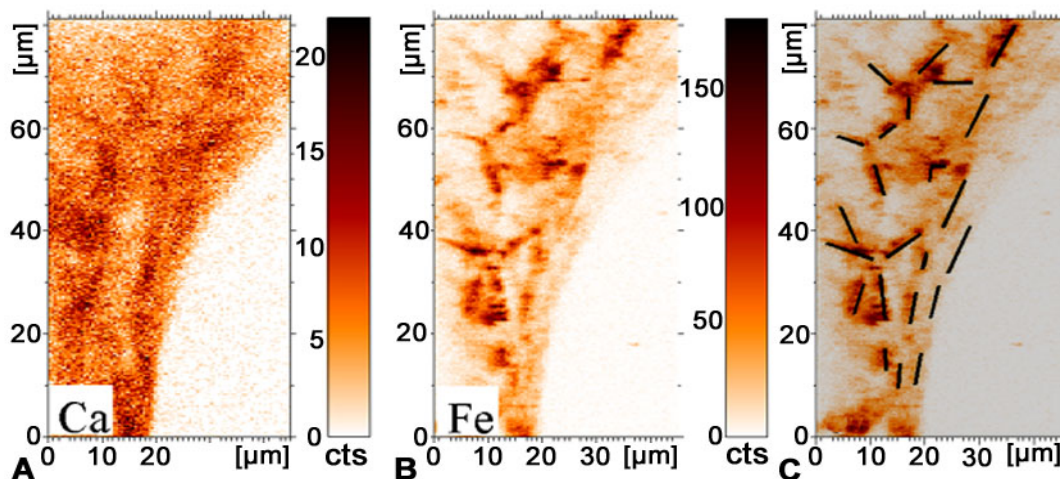


Fig. 2 μ -XRF mappings at ID21 at ESRF (beam size $0.3 \times 1 \mu\text{m}^2$, 1×10^9 ph/s, 7.5 keV). Iron maps with submicrometer lateral resolution reveal structures within the dendritic field, where Ca (Fig. 2A) and Fe (Fig. 2B) are strictly colocalized in a quantity above background level. Fig. 2C: The orientation of these structures which we suggest to assign to individual dendrites (indicated by black bars) scatters around a main direction of the axon bundle. [30 μm thick paraffin section, unstained].

3. Acknowledgement. The project has received grants of the DFG (Fl 177/15-1, 16-1), of HASYLAB (I-05-94, I-05-95), of ESRF (EC-159), of the Freunde und Förderer der Goethe-University Frankfurt and the Stiftung Polytechnische Gesellschaft Frankfurt. The general regulations, policies, and principles given in the "Guide for the Care and Use of Laboratory Animals" were followed.

4. References

- [1] Fleissner Ge. et al. 2003 *J. Comp. Neurol.* **458** 350-360
- [2] Stahl B et al 2007 *HASYLAB Ann Report 2006 (DESY)* 1338-1339
- [3] Fleissner Ge et al 2007 *Naturwissenschaften* **94** 631-642
- [4] Fleissner Ge et al 2007 *J. Ornithol.* **148** 643-648
- [5] Thalau P et al 2007 *Naturwissenschaften* **84** 813-819
- [6] Wiltschko R and Wiltschko W 2006 *Bioessays* **28** 157-168
- [7] Solov'yov A and Greiner W 2007 *Biophys. J.* **93** 1493-14509